JOURNAL OF SPACECRAFT AND ROCKETS
Vol. 32, No. 3, May–June 1995

Dual-Fuel Propulsion in Single-Stage Advanced Manned Launch System Vehicle

Roger A. Lepsch Jr.* and Douglas O. Stanley*
NASA Langley Research Center, Hampton, Virginia 23681-0001
and
Resit Unal†
Old Dominion University, Norfolk, Virginia 23529

As part of the United States Advanced Manned Launch System study to determine a follow-on, or complement, to the Space Shuttle, a reusable single-stage-to-orbit concept utilizing dual-fuel rocket propulsion has been examined. Several dual-fuel propulsion concepts were investigated. These include: a separate-engine concept combining Russian RD-170 kerosene-fueled engines with space shuttle main engine-derivative engines; the kerosene- and hydrogen-fueled Russian RD-701 engine; and a dual-fuel, dual-expander engine. Analysis to determine vehicle weight and size characteristics was performed using conceptual-level design techniques. A response-surface methodology for multidisciplinary design was utilized to optimize the dual-fuel vehicles with respect to several important propulsion-system and vehicle design parameters in order to achieve minimum empty weight. The tools and methods employed in the analysis process are also summarized. In comparison with a reference hydrogen-fueled single-stage vehicle, results showed that the dual-fuel vehicles were from 10 to 30% lower in empty weight for the same payload capability, with the dual-expander engine types showing the greatest potential.

Nomenclature

Al-Li	= aluminum-lithium
b	= equation coefficient
g	= acceleration of gravity, 32.2 ft/s^2
gg	= gas generator
H_2	= hydrogen
HC	= hydrocarbon
I_s	= specific impulse, s
$(LH_2)_{fr}$	= LH_2 mass flow rate fraction of total propellant mass flow rate
LH_2	= liquid hydrogen (at 4.43 lb/ft^3)
LO_2	= liquid oxygen (at 71.2 lb/ft^3)
M_{tr}	= transition Mach number
n	= number of configuration variables
O/F	= oxidizer-to-fuel ratio
O_2	= oxygen
P/L	= payload
P_c	= chamber pressure, psia
sc	= staged combustion
$(T_{HC})_{fr}$	= fraction of lift-off thrust generated by hydrocarbon-fueled engines
T/W	= thrust-to-weight ratio
T/W_G	= thrust-to-gross-weight ratio
T_{sl}	= sea level thrust, lb
T_{vac}	= vacuum thrust, lb
V	= incremental velocity, ft/s
Y	= response-surface value
y	= configuration variable value
ε	= nozzle expansion ratio
ε_{SSME}	= SSME nozzle expansion ratio

Presented as Paper 93-2275 at AIAA/SAE/ASME/ASEE 29th Joint Propulsion Conference, Monterey, CA, June 28–30, 1993; received July 28, 1993; revision received May 11, 1994; accepted for publication July 4, 1994.

*Aerospace Engineer, Space Systems and Concepts Division. Member AIAA.
†Associate Professor, Engineering Management Department.

Introduction

THE United States is examining a number of manned Earth to orbit (ETO) vehicle options to replace or complement the current Space Transportation System under the Advanced Manned Launch System (AMLS) study.[1–3] In order to provide a range of schedule and technology options, a wide variety of vehicle types and propulsion systems have been examined. These include single-stage and two-stage systems, systems utilizing rocket and airbreathing propulsion, systems for personnel and/or cargo transportation, and systems with varying degrees of reusability.[4–6] The AMLS effort is part of a U.S. government study to define systems that meet future mission requirements of transporting personnel and payloads requiring a manned presence, while emphasizing improved cost-effectiveness, increased vehicle reliability, and large operational margins. The goals of the AMLS study are to examine systems that provide routine, low-cost manned access to space. Technologies and system approaches are being studied that will contribute to significant reductions in operating costs relative to current systems.[7] The single-stage vehicle presented in this paper would be expected to have a 2005–2010 initial operating capability (IOC) in order to replace an aging Shuttle fleet. Hence, a 1995–2000 technology readiness date has been assumed to represent normal growth (evolutionary) technology advances in vehicle structure, propulsion, and subsystems. Although many of these assumed technological advances contribute to significant weight savings in the vehicle, a portion of them have been applied to provide aspects of vehicle design that enhance the operations, reliability, and safety of the system.

The introduction of a reusable single stage vehicle (SSV) into the U.S. launch-vehicle fleet early in the next century could greatly reduce ETO launch costs. Currently, the AMLS study is concentrating on the design and evaluation of winged, rocket-powered, single-stage vehicles to transport 20 klb of payload and two crew to and from the Space Station Freedom (SSF). Such an SSV could also be used for SSF personnel transport and would eliminate the need to develop, produce, and maintain two dissimilar vehicles as required by two-stage systems. The conceptual design of an SSV using a wide variety of evolutionary technologies is presented in Ref. 8. The propulsion system for this vehicle consisted of engines derived from the liquid-hydrogen–liquid-oxygen SSME. This paper focuses on the effects of applying dual-fuel rocket propulsion to this vehicle concept. Numerous studies[9–17] have shown that

significant empty-weight and size reductions of single-stage vehicles are possible when liquid-hydrocarbon–liquid-oxygen (LHC-LO_2) propulsion is combined with liquid-hydrogen–liquid-oxygen (LH_2-LO_2) propulsion. The use of hydrocarbon fuel in addition to hydrogen fuel reduces vehicle size and empty weight by increasing propellant bulk density and propulsion system thrust-to-weight ratio at the expense of overall propulsion system specific impulse.

Several dual-fuel propulsion concepts are examined in this paper. These include: a separate-engine concept combining existing Russian RD-170 kerosene-fueled engines with SSME-derivative engines; the kerosene- and hydrogen-fueled Russian RD-701 engine; and a dual-fuel, dual-expander engine.[16–18] Analysis to determine vehicle weight and size characteristics was performed using conceptual-level design techniques. Comparisons were made with respect to a reference hydrogen-fueled SSV of the same configuration, mission capability, and technology level. To examine the effects of engine and vehicle design parameter variations and to determine the optimum values for minimum vehicle empty weight, a response-surface methodology for system optimization was utilized.[19] The design and analysis of the AMLS SSV was facilitated by the use of state-of-the-art computer design tools in a variety of disciplines. These tools and the methods employed in the analysis process are also summarized as a part of this paper.

Analysis Methods

Conceptual Vehicle Design

The physical characteristics of the vehicle were determined through a conceptual analysis involving trajectory, weights/sizing, geometry, and aerodynamics. All of the trajectory analysis for the AMLS single-stage vehicle was performed using the three-degree-of-freedom Program to Optimize Simulated Trajectories (POST). POST is a generalized point-mass, discrete-parameter targeting and optimization program which allows the user to target and optimize point-mass trajectories for a powered or unpowered vehicle near an arbitrary rotating, oblate planet.[20] The weights/sizing analysis was performed using the NASA-developed Configuration Sizing (CONSIZ) weights/sizing package. CONSIZ provides the capability of sizing and estimating weights for a variety of aerospace vehicles using mass-estimating relations based on historical regression, finite-element analysis, and technology level. All of the geometry and subsystem packaging of the AMLS SSV was performed using the NASA-developed Solid Modeling Aerospace Research Tool (SMART) geometry package. SMART is a menu-driven interactive computer program that provides three-dimensional Bézier-surface representations of aerospace vehicles for use in configuration design, aerodynamic analysis, and structural analysis.[21] The Aerodynamic Preliminary Analysis System (APAS) was used to determine vehicle aerodynamics. In the subsonic and low supersonic speed regimes, APAS utilizes a combination of slender-body theory, viscous- and wave-drag empirical techniques, and source and vortex panel distributions to estimate the vehicle aerodynamics. At high supersonic and hypersonic speeds, a noninterference finite-element model of the vehicle is analyzed using empirical impact pressure methods and approximate boundary-layer methods.[22] Figure 1 demonstrates the iterative process required between these various disciplines to obtain a vehicle point design.

Optimization Technique

The parametric optimization of the AMLS single-stage configuration employs a response surface methodology (RSM) originally developed by Box and Wilson.[19] The RSM utilizes central composite design (CCD) to efficiently characterize a parameter space using statistically selected experiments (or configurations). CCD employs orthogonal arrays from design-of-experiments theory to study a parameter space, which usually has a large number of decision variables, with a relatively small number of experiments (or configurations).[23,24] Reference 25 summarizes an application of first-order Taguchi methods to launch-vehicle parametric design and optimization. CCD is a second-order extension of these methods. It

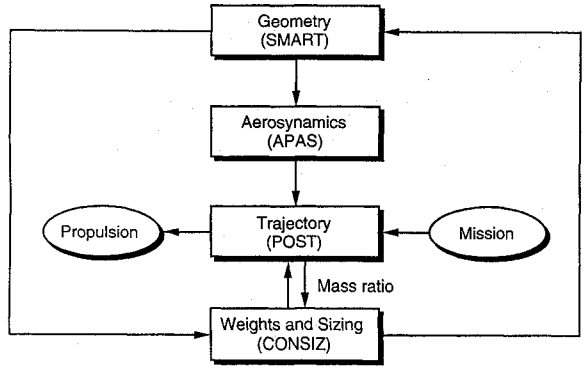

Fig. 1 AMLS vehicle design process.

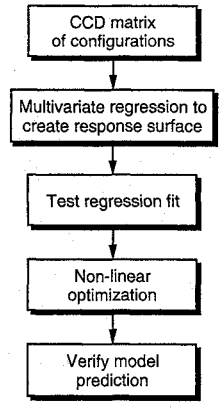

Fig. 2 Response surface methodology.

utilizes first-order models, augmented by $2n + 1$ additional experiments (where n is the number of parameters to be varied), to allow estimation of the coefficients b of a second-order response surface model of the type

$$Y = b_0 + \sum b_i y_i + \sum b_{ii} y_i^2 + \sum \sum b_{ij} y_i y_j$$

For this application, Y could be the vehicle weight, and each y could be a vehicle parameter to be varied. Construction of a second-order model requires that each design parameter be varied over at least three levels (or values) to allow estimation of the equation coefficients. A full factorial design process would require 3^n experiments. Reference 25 demonstrates that the required number of experiments can be greatly reduced by employing fractional factorial design methods like those of Taguchi. However, the number of experimental point designs needed for fitting a second-order model using CCD is significantly less than required by Taguchi's orthogonal arrays or by full factorial designs. For example, a problem involving five parameters would require only 27 experiments using CCD, as opposed to 81 required by Taguchi's method and 243 required by a full factorial design study.

The RSM design and optimization method used in the study is shown in Fig. 2. The use of CCD, multivariate regression, and nonlinear optimization techniques forms the basis of RSM.[26] The CCD element is used to efficiently determine the multivariate design parameter combinations needed for analysis. The resulting data are then analyzed using regression analysis techniques to determine the output response surface as a function of the input parameters. The resulting generalized response-surface equation is then statistically analyzed for lack of fit. The optimum parameters values are then determined using nonlinear optimization techniques to analyze the second-order response surface. A verification experiment is then performed to determine the predictive capability of the model. This methodology allows rapid exploration of the parameter space and determination of sensitivities. The regression and optimization analysis can be performed efficiently using conventional spreadsheet software.

Vehicle Description

Mission and Guidelines

The design reference mission for the AMLS single-stage vehicle is to deliver to the SSF and return a 20-klb payload and two crew when launched from the Eastern Test Range at the Kennedy Space Center (KSC). The vehicle is designed to support the two crew for a 5-day mission duration. Additional personnel (four to six) and consumables could be accommodated in a SSF crew rotation module located in the payload bay. The vehicle is designed to be flown with crew only when necessary and could be flown in an unmanned mode. The payload bay is 15 ft in diameter and 30 ft long. Following launch insertion into a 50- by 100-n.mi. orbit, on-board maneuver propellant would provide an incremental velocity (ΔV) of 1100 ft/s to achieve a circular orbit with a 220-n.mi. altitude and inclination of 28.5 deg. A 100-ft/s maneuver capability is included in this total for SSF proximity operations. Landing would nominally be at the KSC launch site. Examinations of recent mission models of future ETO transportation requirements indicate that a vehicle with these capabilities can capture a very large portion of future civil, military, and commercial payloads.[27–29]

The SSV was required to have a 1100-n.mi. crossrange capability to allow once-around abort for launch to a polar orbit and to increase daily landing opportunities to selected landing sites. The SSV is also required to have a full range of intact abort opportunities in the event of a forced shutdown of a single main engine. Crew and passenger escape is provided by ejection seats in the appropriate portions of the flight regime. An escape module is not considered necessary for the current single-engine-out abort scenario. All vehicle trajectories have maximum acceleration limits of 3 g and normal load constraints equivalent to a 2.5 g subsonic pullup maneuver. In the design of the AMLS SSV, a 15% empty-weight growth margin was allocated.

Reference Hydrogen-Fueled Configuration

All configurations examined in this study are derived from the hydrogen-oxygen SSV configuration of Ref. 8, which is a vertical-takeoff, horizontal-landing winged vehicle with a circular-cross-section fuselage for structural efficiency. In Ref. 8, a number of configuration trade studies were performed to optimize the geometry of the vehicle with respect to empty weight while satisfying constraints on landing velocity and on subsonic, supersonic, and hypersonic trim and stability. This geometry was utilized in determining a reference hydrogen-fueled vehicle for comparison with the dual-fuel vehicle concepts. Figure 3 shows the reference hydrogen-fueled SSV. The payload bay is located between the LO_2 and LH_2 tanks and is integrated with an aerodynamic fairing. An airlock/workstation located aft of the crew cabin provides crew access to the payload bay and to the SSF through a hatch on top. The vehicle employs a standardized payload canister with common interfaces to allow off-line processing of payloads and rapid payload integration. The vehicle employs wingtip fins rather than a single vertical tail. The fins provide directional control but are insufficient in size to provide static directional stability. The propulsion system utilizes seven SSME-derivative engines, each with an expansion ratio of 50 and a throttle setting of 104%. This gives the vehicle a liftoff thrust-to-weight ratio T/W of 1.2.

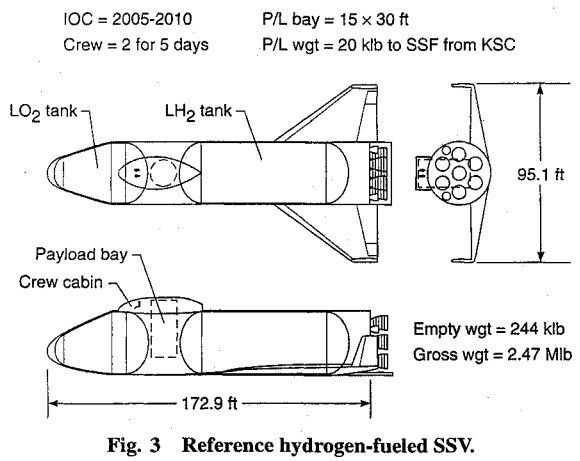

Fig. 3 Reference hydrogen-fueled SSV.

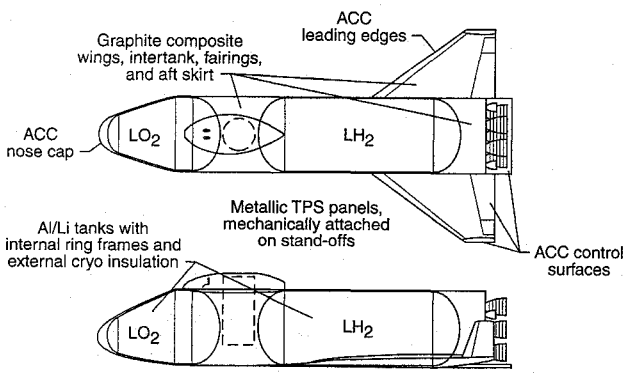

Fig. 4 SSV material assumptions.

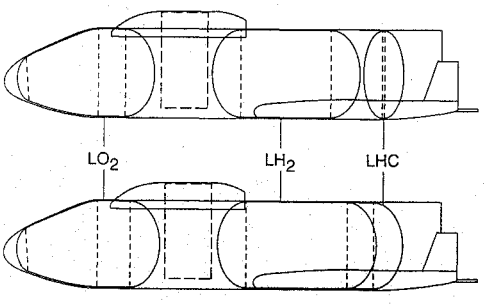

Fig. 5 Dual-fuel configuration options.

Figure 4 shows the major material and structural technologies for the SSV. The structural design utilizes integral propellant tanks constructed to aluminum-lithium alloy 2095 and a nose, intertank, aft body, and wing constructed of graphite-polyetheretherketone (PEEK) composite. The insulation utilized for the cryogenic propellant tanks is an external closed-cell foam. The thermal protection system covering the vehicle is composed of a combination of advanced carbon-carbon (ACC), inconel, and titanium panels. All aerodynamic control surfaces are of an ACC hot-structure design. These evolutionary material and subsystem technologies are consistent with an initial operating capability of 2005–2010. As shown in Fig. 3, the resulting total empty weight with the above assumptions is 244,000 lb, and the gross weight is 2,470,000 lb.

Dual-Fuel Configurations

Two dual-fuel variations of the reference hydrogen-fueled vehicle were investigated in this study and are shown in Fig. 5. The two concepts differ only in the arrangement of the propellant tanks. The top configuration in the figure has a separate LHC propellant tank located aft of the LH_2 propellant tank. This requires an additional intertank structure. The bottom configuration in the figure employs a common bulkhead between the LH_2 and LHC tanks, which eliminates the intertank and improves the propellant volume packaging efficiency. Although this common-bulkhead approach reduces the vehicle empty weight compared with the separate-tank configuration, the use of a common bulkhead in a reusable vehicle raises reliability and inspectability concerns that require further study. Therefore, the separate-tank configuration is currently considered preferable to reduce risk and operational complexity.

Propulsion Systems

Two general approaches to dual-fuel propulsion were investigated in this study. The first approach utilizes a combination of separate engines, each burning either hydrogen fuel or hydrocarbon fuel, while the second approach utilizes dual-fuel engines capable of burning both hydrogen and hydrocarbon fuels simultaneously and hydrogen fuel individually. In both the separate engine and dual-fuel engine approaches, improvements in propellant bulk density over an all-hydrogen-fueled vehicle are achieved by utilizing high-density hydrocarbon fuel to reduce the requirement for low-density hydrogen. Hydrocarbon fuels such as kerosene and propane have over 10 times

Table 1 RD-170 engine performance characteristics

T_{sl}, lb	1,632,000
T_{vac}, lb	1,777,000
Sea level I_s, s	309
Vacuum I_s, s	337
Cycle	staged combustion
P_c, psia	3,560
O/F	2.6
Weight (including gimbal actuators), lb	26,575

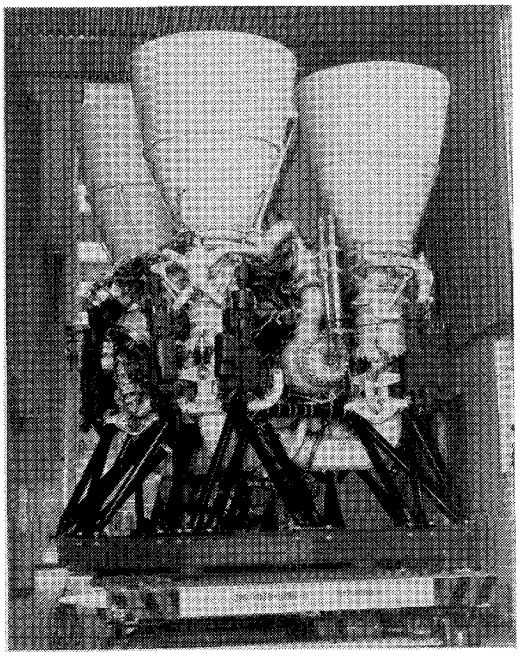

Fig. 6 RD-170 kerosene-oxygen engine.

the density of liquid hydrogen. This high propellant bulk density is achieved at the expense of specific impulse. However, it allows a reduction in propellant tank volume for a given propellant weight, which has a favorable effect on vehicle sizing. Improved sea-level engine T/W with the use of low-expansion-ratio hydrocarbon engines is also a major contributor to better overall performance. With dual-fuel engines, an additional benefit is obtained from the reduction in propulsion-system weight that can be achieved relative to separate engines, partly due to the use of a common nozzle.

For the separate-engine approach, the RD-170 hydrocarbon engine and a planned derivative of the hydrogen-fueled SSME were used. The RD-170 is a high-chamber-pressure, high-performance engine built by NPO Energomash of Russia and currently in use on a number of Russian launch vehicles. This engine (pictured in Fig. 6) utilizes oxygen and kerosene propellants, which feed into four separate thrust chambers. Table 1 shows the performance characteristics of the RD-170. The SSME-derivative engine used in this study differs from the current SSME in a number of ways, which are intended to enhance the reliability and operability of the engine. Extended-life, high-pressure turbopumps are utilized with hydrostatic bearings. Electromechanical actuators are used for gimbals and valves. Other improvements include a two-duct hot gas manifold, Block II controller, and integrated health monitoring. A larger throat in the combustion chamber is also utilized, which results in a small performance gain.[30] Table 2 shows the characteristics of the derivative SSME for a number of nozzle expansion ratios. A 104% throttle setting was used to provide a consistent comparison with the reference hydrogen-fueled SSV. However, it should be noted that higher engine throttle settings adversely affect engine reliability, and that a lower throttle setting would be preferable.

The flight operations scenario for the RD-170/SSME vehicle assumes that both engine types are operated in a parallel-burn mode from liftoff through some transition Mach number, where the RD-170 engines are shut down. Previous studies have shown that parallel burning of separate hydrocarbon-fueled and hydrogen-fueled engines results in lower vehicle empty weight than burning the engines in series.[12,13]

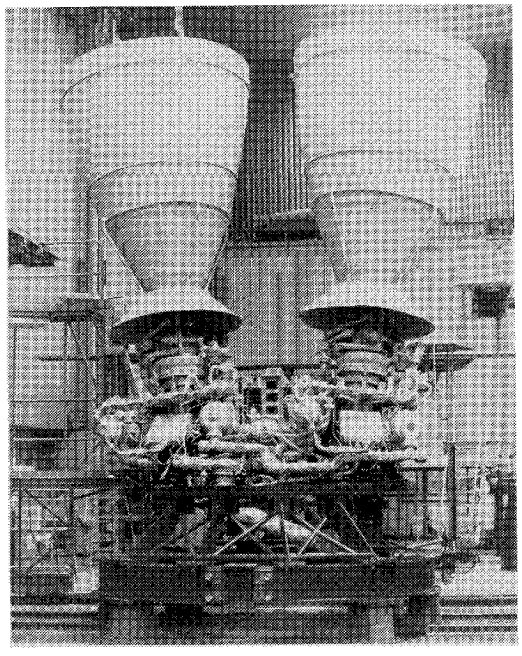

Fig. 7 RD-701 dual-fuel engine mock-up.

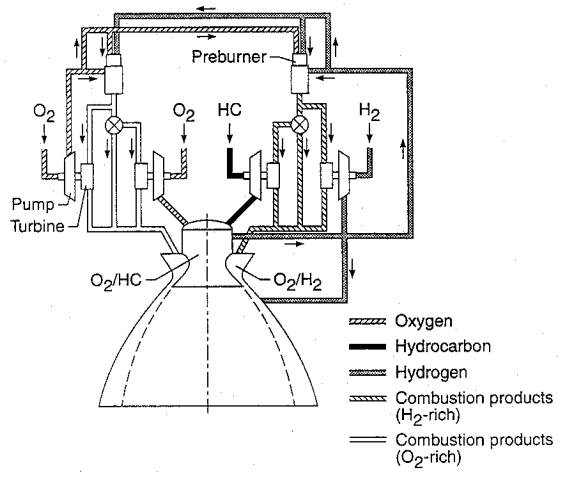

Fig. 8 Schematic of dual-fuel, dual-expander engine.

For the dual-fuel engine approach, two different engine concepts were examined: the RD-701 engine and a dual-fuel, dual-expander engine. The RD-701 engine is currently under study by NPO Energomash, with support from Pratt & Whitney of the U.S. A picture of the mockup is shown in Fig. 7. The RD-701 engine is a reusable, mixed-combustion engine consisting of two separate and identical thrust-chamber assemblies capable of burning a combination of LH_2, LO_2, and kerosene. A pair of turbopumps for each thrust chamber feed the propellants. The engine is designed to operate in a dual-fuel mode initially and then transition to a single-fuel mode (LH_2-LO_2) later in flight. The design of the RD-701 engine is based on proven design concepts from the existing RD-170 engine. Performance characteristics for this engine concept are summarized in Table 3. The dual-fuel, dual-expander engine has been studied extensively for use on single-stage launch vehicles.[16,17] A general schematic of this engine type is shown in Fig. 8. It combines hydrogen and hydrocarbon combustion within the same engine using coannular combustion chambers, which exhaust through a common nozzle. The outer chamber burns oxygen and hydrogen while the inner chamber burns oxygen and a hydrocarbon fuel. As with the RD-701, the engine operates initially in a dual-fuel mode, where both hydrocarbon and hydrogen are burned,

Table 2 SSME-derivative engine performance characteristics (104 percent power level)

Expansion ratio	40	50	60	70	77.5
T_{sl}, lb	428,800	420,000	410,100	399,600	391,900
T_{vac}, lb	478,500	482,200	484,700	486,700	488,300
Sea level I_s, s	397.4	389.2	380.1	370.3	363.3
Vacuum I_s, s	443.6	447.0	449.3	451.2	452.7
P_c, psia	3,126	3,126	3,126	3,126	3,126
O/F	6	6	6	6	6
Weight, lb	6,629	6,780	6,933	7,087	7,203

Table 3 RD-701 engine performance characteristics

Mode	1	2
Propellants	LO_2-LH_2-RP-1	LO_2-LH_2
T_{sl}, lb	714,000	N/A
T_{vac}, lb	900,000	357,000
Sea level I_s, s	330	N/A
Vacuum I_s, s	415	460
Cycle	staged combustion	staged combustion
P_c, psia	4,266	1,792
Propellant mixture	81.4% LO_2, 12.6% RP-1, 6% LH_2	6(O/F)
Expansion ratio	123.4	123.4
Weight, lb	9,742	9,742

Note: weight includes boost pumps, gimbal actuators, thrust frame, thermal protection, and sensors.

Table 4 Dual-expander engine performance characteristics

Mode	1	2
Propellants	LO_2-C_3H_8-LH_2	LO_2-LH_2
T_{sl}, lb	666,700	N/A
T_{vac}, lb	750,000	235,100
Sea level I_s, s	341	N/A
Vacuum I_s, s	383.7	462.9
Cycle	gg/sc (C_3H_8/LH_2)	staged combustion
P_c, psia	5,000/2500 (C_3H_8/LH_2)	2,500
O/F	3.2/6 (C_3H_8/LH_2)	6
Expansion ratio	74.8/36.3 (C_3H_8/LH_2)	119.9
Weight, lb	8,127	8,127

and then transitions to a single-fuel mode where only hydrogen is burned. During the single-fuel mode, the nozzle expansion ratio is effectively increased due to the reduction in throat area when the hydrocarbon chamber is inoperative. This results in high performance at altitude. A number of hydrocarbon propellant types have been investigated for use in this concept; subcooled liquid propane was selected for this study in view of results showing that lower vehicle empty weight can be achieved with this hydrocarbon fuel than with other common ones.[14,17] Table 4 shows the estimated performance characteristics of this engine when designed to deliver a vacuum thrust of 750,000 lb in the dual-fuel mode.[18] A gas generator cycle is assumed for the hydrocarbon portion of the engine, and a staged combustion cycle is assumed for the hydrogen portion.

The LH_2 and LO_2 propellants utilized by these concepts are assumed to be contained within the vehicle at normal boiling point (NBP) conditions. The densities of NBP LH_2 and LO_2 are 4.43 and 71.2 lb/ft^3, respectively. For RP-1, which was used to approximate kerosene, the density was set at a near-room-temperature value of 50.5 lb/ft^3. The density of liquid propane was fixed at 45.5 lb/ft^3, corresponding to a subcooled temperature equal to the temperature of NBP LO_2 (−297°F).

Vehicle Optimization and Trades

To determine the physical characteristics of the dual-fuel SSVs and the effects of propulsion-system and design parameter variations, the analysis methods described above were utilized. The optimization process described above was performed on the separate-tank dual-fuel configuration. It was assumed that the values of the parameters obtained from the optimization of this configuration would be approximately the same for the common-bulkhead configuration. Optimization of vehicle empty weight with respect to one or more design parameters was performed for all dual-fuel SSV concepts. The empty weight of these vehicles was then compared with the hydrogen-fueled reference SSV. Empty weight was selected as the basis of comparison because for the same level of technical complexity, vehicle development costs tend to vary as a function of empty weight. It should be noted that there is an obvious development-cost benefit to utilizing an existing engine over a new engine design. However, quantification of the influence of this on vehicle life-cycle costs requires detailed analysis, which is beyond the scope of this paper.

RD-170/SSME Vehicle Concept

The optimization of vehicle empty weight by the response-surface methodology described above was performed by varying four vehicle design and engine parameters: the liftoff T/W, the RD-170 cutoff Mach number, the RD-170/SSME propulsive-thrust split, and the SSME expansion ratio. Although additional engine parameters could have easily been incorporated into the optimization process, no other parametrics were available at the time of this study. These four parameters were varied over a specified range, within which the optimum values were anticipated to occur. To characterize this parameter space, the CCD methodology described above was utilized. With four parameters, this resulted in a CCD array containing 25 different vehicle cases, each case representing a specific vehicle point design. For each vehicle point design, each of the parameters (liftoff T/W, thrust split, etc.) was held at a value specified by the CCD methodology. Because liftoff T/W was a specified parameter, the number of engines necessary to provide liftoff thrust was allowed to be a noninteger number. To calculate the weight of the engines, total thrust for each engine type was divided by the engine T/W. Characteristics of the RD-170 engine were fixed, but the characteristics of the SSME-derivative engine were dependent on nozzle expansion ratio.

The vehicle point designs required by the CCD methodology were evaluated to obtain empty-weight values using the conceptual design methods described above. A second-order regression fit was then performed on the 25 empty weights, and an equation was obtained relating the empty weight to the four parameters. Unconstrained nonlinear optimization on this equation was performed over the parameter space to obtain the values of the parameters that result in minimum vehicle empty weight. A final vehicle point design using the parameters obtained was evaluated to verify the results.

The results of the optimization for this vehicle concept are shown in Table 5. The empty weight from the verification agrees with the predicted empty weight to within 1.5%. The difference is largely caused by the error from the second-order regression-fit approximation of the actual empty weight. The verified empty-weight value of 219,800 lb is approximately 10% lower than the empty weight of the hydrogen-fueled reference SSV. If the common-bulkhead configuration is utilized, this increases to 16%. As shown in the table, the liftoff T/W was driven to the low-bound value of 1.2, and the hydrocarbon-engine thrust fraction was driven to the high-bound value of 0.75. The liftoff T/W selection was not allowed to be less than 1.2, to provide performance margin for a controlled abort maneuver in the event of partial loss of thrust due to engine malfunction. With a liftoff T/W of 1.2 and a gross weight determined to be 2,830,000 lb, the separate-tank configuration requires 1.56 RD-170 engines and 2.11 SSME-derivative engines having an expansion ratio of 68. Table 6 shows the performance characteristics of the SSME-derivative engine with this expansion ratio.

Figure 9 shows the sensitivity of the empty weight to the individual parameters, using the equation for empty weight determined by the RSM. Only positive variations in liftoff T/W and only negative

Table 5 RD-170/SSME-vehicle parameter ranges and optimization results

Parameter	Range	Optimized value
$(T_{HC})_{fr}$	0.45–0.75	0.75
T/W_G	1.20–1.40	1.2
ε_{SSME}	40–77.5	68
M_{tr}	4–12	8.6
Predicted empty wt., lb		216,800
Verified empty wt., lb		219,800

Table 6 SSME-derivative engine performance characteristics with optimum ε

Expansion ratio	68
T_{sl}, lb	401,500
T_{vac}, lb	486,300
Sea level I_s, s	372.3
Vacuum I_s, s	450.9
Weight, lb	7,058

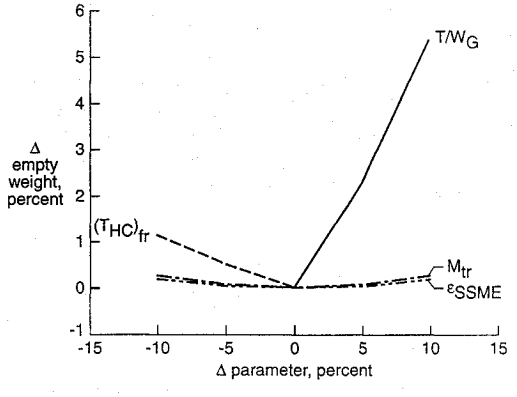

Fig. 9 RD-170/SSME vehicle empty weight sensitivity to parameters.

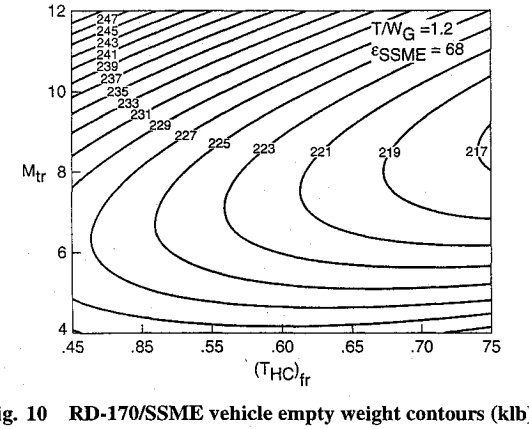

Fig. 10 RD-170/SSME vehicle empty weight contours (klb).

variations in the hydrocarbon thrust fraction were allowed, so as to remain within the range of validity of the empty-weight equation. As shown in the figure, the liftoff T/W is the most significant parameter by a considerable margin. Of the remaining parameters, the fraction of hydrocarbon-engine thrust is the most influential. The effect on empty weight of variations in both SSME expansion ratio and transition Mach number about the indicated optimums is small.

Figure 10 shows empty-weight contours as a function of hydrocarbon-engine thrust fraction and transition Mach number, with the SSME expansion ratio set at the optimum value of 68 and T/W set at the low-bound value of 1.2. This figure shows that in an approximate region bounded by values of transition Mach number ranging from 6 to 10 and values of hydrocarbon-engine thrust fraction ranging from 0.6 to 0.75, the empty-weight variation is relatively small. This allows some flexibility in determining the mix of hydrogen and hydrocarbon-fueled engines without incurring a large empty-weight penalty. Figure 10 also suggests that a slightly higher hydrocarbon-engine thrust fraction may result in an even lower empty weight. However, this is not true. As expressed earlier, the RSM-developed relationship for the empty weight is only an approximation. Therefore, the true optimum point may not be exactly at the point indicated by this analysis. In fact, it was found that by holding all other parameters constant, a lower empty weight was achieved with a hydrocarbon-engine thrust fraction near 0.7, but the weight improvement was less than 1%.

RD-701 Vehicle Concept

The optimization of the RD-701 vehicle empty weight by the response-surface methodology was performed in a similar fashion to the RD-170/SSME vehicle optimization. Four parameters were varied: the liftoff T/W, the dual-fuel to single-fuel transition Mach number, the LH_2 propellant flow-rate fraction in the dual-fuel mode, and the nozzle expansion ratio. As with the previous vehicle optimization, this resulted in the requirement to analyze 25 individual vehicle cases in order to characterize the parameter space sufficiently. A second-order regression fit was then performed on the 25 empty weights, and an equation was obtained relating the empty weight to the four parameters. Unconstrained nonlinear optimization on this equation was performed over the parameter space to obtain the values of the parameters that result in minimum vehicle empty weight. As before, the number of engines was determined from the thrust requirement and was allowed to have a noninteger value. Engine parametrics for the RD-701 as a function of LH_2 propellant flow-rate fraction and nozzle expansion ratio were utilized to obtain engine performance characteristics at the specific values required for the 25 individual vehicle cases. The engine weights utilized in the RSM analysis were considered the best estimates available, but later estimates indicated that these weights were optimistic. In order to show the effect of the engine weight difference, the vehicle resulting from the optimization was adjusted to reflect the later estimates, and both cases are presented in this paper.

The results of the optimization for this vehicle concept are shown in Table 7. To verify the results of the optimization, a final vehicle point design was evaluated using the optimum values of the parameters. The empty weight from the verification is less than 1% different from the predicted empty weight. As shown in the table, both liftoff T/W and LH_2 propellant flow fraction were driven to their respective minimum values. The liftoff T/W limitation was discussed in the previous section and is considered to be nonvariable. However, the limit on the LH_2 propellant flow fraction may require further investigation to determine if a lower value may be optimum. The verified empty-weight value of 160,600 lb, with the initial engine weight estimate, is lower than the reference hydrogen-fueled SSV by 34% (38% in the common-bulkhead configuration). However, when this vehicle is adjusted to account for the later engine weight estimates, the empty weight increases to 189,000 lb for the separate-tank configuration. This is still 23% lower than for the reference SSV. Utilizing a common bulkhead results in a 28% reduction. With a liftoff T/W of 1.2 and a gross weight determined to be 2,300,000 lb, the separate-tank configuration requires 3.77 RD-701 engines. Table 8 shows the performance characteristics of the optimized RD-701 engine with the initial engine weight estimate. The updated engine weight estimate is approximately 26% higher than the weight shown in the table.

Figure 11 shows the sensitivity of empty weight to the individual parameters using the equation for empty weight determined by the

Table 7 RD-701-vehicle parameter ranges and optimization results

Parameter	Range	Optimized value
ε	40–100	65
T/W_G	1.20–1.40	1.20
$(LH_2)_{fr}$, percent	3–6	3
M_{tr}	4–12	8.9
Predicted empty wt., lb		159,200
Verified empty wt., lb		160,600

Table 8 RD-701 engine performance characteristics with optimum parameter values

Mode	1	2
T_{sl}, lb	732,000	N/A
T_{vac}, lb	829,300	349,300
Sea level I_s, s	337.5	N/A
Vacuum I_s, s	382.3	450.2
Propellant mixture	76.8% LO_2, 20.2% RP-1, 3% LH_2	6(O/F)
Expansion ratio	65	65
Weight, lb	8,527	8,527

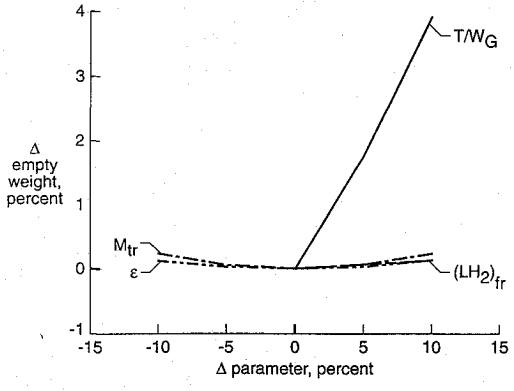

Fig. 11 RD-701 vehicle empty weight sensitivity to parameters.

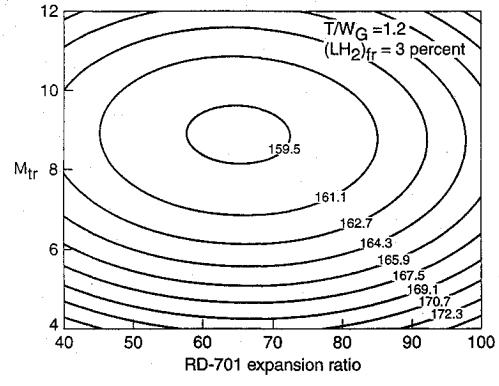

Fig. 12 RD-701 vehicle empty weight contours (klb).

RSM. As shown in the figure, the liftoff T/W is by far the most significant parameter. Only positive variations in liftoff T/W and LH_2 propellant flow fraction were allowed, because negative variations would be outside the range of validity of the empty-weight equation. Of these parameters, only the transition Mach number and the expansion ratio show nonlinear effects. The transition Mach number is slightly more influential than the LH_2 propellant flow fraction and the nozzle expansion ratio.

Figure 12 shows empty-weight contours calculated using the RSM-derived equation. Because both liftoff T/W and LH_2 propellant flow fraction were optimized to the limit values (1.2 and 3%), they were fixed at those values, and the transition Mach number and nozzle expansion ratio were varied. This figure shows that there is little empty-weight sensitivity of these parameters for the ranges shown. This indicates that a great deal of flexibility exists for the choice of nozzle expansion ratio and for the engine mode transition point.

Dual-Expander Vehicle Concept

The dual-fuel, dual-expander engine was not optimized using the response-surface methodology, because of the unavailability of engine parametrics at the time of this study. For the dual-expander engine concept given in Table 4, 70% of the seal-level thrust is generated by the combustion of hydrocarbon fuel, and 30% by the combustion of hydrogen. This thrust split, as well as the nozzle expansion ratio, oxidizer-to-fuel ratios, and chamber pressures shown, was determined from previous studies to give low single-stage-to-orbit vehicle empty weight.[15,17] The parameter varied to optimize the vehicle for this study was the dual-fuel to single-fuel mode transition Mach number. Based on the optimization results of the other vehicle concepts examined in this study, the liftoff T/W was fixed at 1.2. Although other parameter variations were not examined for this concept, it does provide an important point of comparison for the RD-701 dual-fuel engine.

Table 9 Comparison of dual-fuel, separate tank SSV concepts with reference hydrogen-fueled SSV

Vehicle concept	Empty wt., lb	Gross wt., lb	Body length, ft
Reference SSV	244,000	2,470,000	172.9
RD-170/SSME	219,800	2,830,000	161.8
Dual expander	182,000	2,150,000	151.3
RD-701 (initial wt.)	160,600	1,990,000	145.4
RD-701 (updated wt.)	189,000	2,300,000	151.6

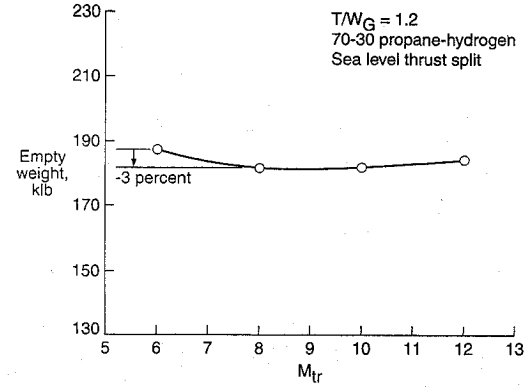

Fig. 13 Effect of transition Mach number on dual-expander vehicle empty weight.

Figure 13 shows the results of the transition Mach-number trade. The sensitivity of the empty weight to the transition Mach number is not great over the range of variation. Therefore, a transition Mach number of 8 was selected as being near optimum with respect to empty weight. This vehicle has an empty weight of 182,000 lb, which is 25% lower than the reference hydrogen-fueled SSV. Utilizing the common-bulkhead configuration results in a 30% decrease in the empty weight. With a liftoff T/W of 1.2 and a gross weight determined to be 2,150,000 lb, the separate-tank configuration requires 3.87 engines of the size listed in Table 4.

Comparison of Concepts

Table 9 shows dimensional and weight characteristics of the dual-fuel, separate-tank SSV concepts in comparison with the reference hydrogen-fueled SSV. All concepts show significant empty weight and size reductions. Among the dual-fuel engine concepts, the RD-701 vehicle with the updated engine weight is very similar to the dual-expander vehicle. Although the dual-expander vehicle was not optimized to the same degree, this does indicate that there may be little to choose between the two engine types.

In terms of safety and cost, a desirable feature for any launch vehicle is to have the capability to abort an ascent without the loss of crew, cargo, or vehicle. An abort analysis has been performed on a configuration very similar to the reference seven-engine SSV to illustrate the capability of intact vehicle recovery any time from liftoff to orbit insertion in the event of a single engine shutdown.[31] This capability would be lacking in the RD-170/SSME, since the loss of an RD-170 engine would represent too large a loss of thrust. Therefore, a higher premium would need to be placed on engine reliability. The RD-701 vehicle also suffers from this problem, as does any vehicle using a small number of large engines. However, unlike the RD-170 engine, the RD-701 engine has separate turbopumps for each thrust chamber. For the vehicle concept presented in this paper, approximately four RD-701 engines were required. This represents an eight-thrust-chamber configuration, one more than in the reference hydrogen-fueled SSV. If the RD-701 engine can be

operated with one thrust chamber shut down, then this will allow an abort similar to the reference SSV.

If consideration is to be given to the development of a new engine such as the RD-701 or the dual-expander, then consideration should also be given to a new hydrogen-fueled engine. A number of new high-performance hydrogen-fueled engines have been proposed in recent years and were not considered in this study. However, a comparison of the dual-fuel vehicle concepts with a hydrogen-fueled SSV utilizing an engine more advanced than the SSME is warranted. Also, before any decisions on preferred propulsion-system type can be made for vehicles of this type, a more detailed vehicle and life-cycle cost analysis is necessary.

Summary

A reusable single-stage-to-orbit vehicle concept utilizing dual-fuel rocket propulsion has been examined as part of the United States Advanced Manned Launch System (AMLS) study to determine a follow-on, or complement, to the Space Shuttle. Several dual-fuel propulsion concepts were investigated. These included: a separate-engine concept combining Russian RD-170 kerosene-fueled engines with SSME-derivative engines; the kerosene and hydrogen-fueled Russian RD-701 engine; and a dual-fuel, dual-expander engine. The separate-engine concept operated the RD-170 and SSME engines in a parallel-burn mode at liftoff and then transitioned in flight to SSME power only. The other two concepts operated in a dual-fuel mode initially and then transitioned to a hydrogen-fuel mode later in flight. A response-surface methodology for multidisciplinary design was utilized to optimize the dual-fuel vehicle concepts with respect to several important propulsion-system and vehicle design parameters in order to achieve minimum empty weight. Comparisons were made with respect to a reference all-hydrogen-fueled SSV of the same configuration, mission capability, and technology level. Two dual-fuel variations of the reference hydrogen-fueled configuration were investigated: a configuration with propellant contained in physically separate tanks and a configuration having the same external shape, but employing a common bulkhead between the fuel tanks.

For the concept employing separate RD-170 and SSME-derivative engines, the empty weight in comparison with that of the reference hydrogen-fueled SSV was 10% less when the separate-tank configuration was utilized and 16% less when the common-bulkhead configuration was utilized. Parameters varied for the optimization were the liftoff T/W, the RD-170 cutoff Mach number, the RD-170/SSME propulsive-thrust split, and the SSME expansion ratio. Results of the optimization showed that little weight is saved by altering the expansion ratio of the SSME nozzle. Results of the optimization also showed that because of low empty-weight sensitivity in the optimum region of the parameters, some flexibility exists in the choice of engine thrust splits and in the RD-170 cutoff Mach number.

In comparison with the reference SSV, the RD-701 vehicle was shown to reduce empty weight by 23% using the separate-tank configuration and 28% using the common-bulkhead configuration. Parameters varied for the optimization were the liftoff T/W, the dual-fuel to single-fuel transition Mach number, the LH_2 propellant flow-rate fraction in the dual-fuel mode, and the nozzle expansion ratio. Results of the optimization showed that the empty-weight sensitivity to the liftoff T/W was high, but that the sensitivity was much lower to the other parameters, allowing considerable range in the choice of values for those parameters.

For the dual-fuel, dual-expander concept, engine parameters were fixed, but a trade study varying the dual-fuel-mode to single-fuel-mode transition Mach number was performed. This resulted in empty-weight reductions compared to the reference SSV of 25% using the separate-tank configuration and 30% using the common-bulkhead configuration. These results match closely with those obtained with the RD-701 dual-fuel engine concept.

The use of hydrocarbon fuel in addition to hydrogen fuel reduces vehicle size and empty weight by increasing the propellant bulk density and propulsion system thrust-to-weight ratio at the expense of the overall propulsion-system specific impulse. Results of this paper show that significant reductions in SSV empty weight are possible with respect to the reference SSME-powered SSV, which may indicate reduced development costs. However, several new hydrogen-fueled engines have been proposed that are more advanced than the SSME. Comparisons of the dual-fuel SSV concepts with an SSV utilizing these new hydrogen-fueled engines was not performed in this paper. The reductions in empty weight might then not be as significant. Also, the use of dual-fuel propulsion increases the complexity of the vehicle relative to the use of single-fuel propulsion, and the effect this has on the operations cost must be quantified.

References

[1]Freeman, D. C., Wilhite, A. W., and Talay, T. A., "Advanced Manned Launch System Study Status," International Astronautical Federation, Paper 91-193, Oct. 1991.

[2]Stanley, D. O., Talay, T. A., Lepsch, R. A., Morris, W. D., and Wurster, K. E., "Conceptual Design of a Fully Reusable Manned Launch System," *Journal of Spacecraft and Rockets*, Vol. 29, No. 4, 1992, pp. 529–537.

[3]Stone, H. W., and Piland, W. M., "An Advanced Manned Launch System Concept," International Astronautical Federation, Paper 92-0870, Aug. 1992.

[4]Piland, W. M., and Talay, T. A., "Advanced Manned Launch System Comparisons," International Astronautical Federation, Paper 89-221, Oct. 1989.

[5]Freeman, D. C., Talay, T. A., Stanley, D. O., and Wilhite, A. W., "Design Options for Advanced Manned Launch Systems," AIAA Paper 90-3816, Sept. 1990.

[6]Stanley, D. O., Engelund, W., Wilhite, A. W., and Laube, J., "A Comparison of Single-Stage and Two-Stage Airbreathing Launch Vehicles at High Staging Mach Numbers," *Journal of Spacecraft and Rockets*, Vol. 29, No. 5, 1992, pp. 735–740.

[7]Talay, T. A., and Morris, W. D., "Advanced Manned Launch Systems," *Proceedings of the 2nd European Aerospace Conference on Progress in Space Transportation*, European Space Agency, SP-293, May 1989, pp. 117–127.

[8]Stanley, D. O., Engelund, W. C., Lepsch, R. A., McMillin, M., Wurster, K. E., Powell, R. W., Guinta, A. A., and Unal, R., "Rocket-Powered Single-Stage Vehicle Configuration Selection and Design," AIAA Paper 93-1053, Feb. 1993.

[9]Salkeld, R., "Mixed-Mode Propulsion for the Space Shuttle," *Astronautics and Aeronautics*, Vol. 9, No. 8, 1971, pp. 52–58.

[10]Salkeld, R., "Contributions to the Discussion of Mixed-Mode Propulsion and Reusable One-Stage-to-Orbit Vehicles," System Development Corporation, Santa Monica, CA, Oct. 1972.

[11]Salkeld, R., and Skulsky, R. S., "Air Launch for Space Shuttles: Impact of Mixed-Mode Propulsion and Comparison with Single-Stage-to-Orbit," System Development Corporation, SP-3788, Santa Monica, CA, Sept. 1974.

[12]Martin, J. A., and Wilhite, A. W., "Dual-Fuel Propulsion: Why it Works, Possible Engines, and Results of Vehicle Studies," AIAA Paper 79-878, May 1979.

[13]Wilhite, A. W., "Optimization of Rocket Propulsion Systems for Advanced Earth-to-Orbit Shuttles," *Journal of Spacecraft and Rockets*, Vol. 17, No. 2, 1980, pp. 99–104.

[14]Martin, J. A., "Hydrocarbon Rocket Engines for Earth-to-Orbit Vehicles," *Journal of Spacecraft and Rockets*, Vol. 20, No. 3, 1983, pp. 249–256.

[15]Gaynor, T. L., and Cervisi, R. T., "Effects of Propulsion System Performance and Technology Level on an Advanced Military Launch Vehicle," AIAA Paper 84-1225, June 1984.

[16]Beichel, R., "The Dual Expander Engine—Key to Economical Space Transportation, *Astronautics and Aeronautics*, Vol. 15, Nov. 1977, pp. 44–51.

[17]Hyde, J. C., Chen, F. F., Nguyen, T. V., Vice, D. D., and O'Brien, C. J., "Dual Expander Engine Thrust Chamber Technology," Final TR 86C0113-F, Aerojet TechSystems Company, Sacramento, CA, March 1989.

[18]Devereux, G. B., Bair, E. K., and Lacefield, T. C., "Space Transportation System Main Engine Study—Part 2: Single-Stage-to-Orbit Engine Characterization Study," Aerojet TechSystems Company, Contract NAS8-36867, Sacramento, CA, Jan. 1987.

[19]Myers, R. H., *Response Surface Methodology*, Allyn and Bacon, Boston, 1971.

[20]Braur, G. L., Cornick, D. E., and Stevenson, R., "Capabilities and Applications of the Program to Optimize Simulated Trajectories (POST)," NASA CR-2770, Feb. 1987.

[21]McMillin, M. L., et al., "A Solid Modeler for Aerospace Vehicle Preliminary Design," AIAA Paper 87-2901, Sept. 1987.

[22]Divan, P. E., "Aerodynamic Analysis System for Conceptual and Preliminary Analysis from Subsonic to Hypersonic Speeds," AIAA Paper 80-1897, Aug. 1980.

[23]Montgomery, D. C., *Design and Analysis of Experiments*, Wiley, Newark, NJ, 1991.

[24]Khuri, A. I., and Cornell, J. A., *Response Surfaces: Designs and Analyses*, Marcel Dekker, New York, 1987.

[25]Stanley, D. O., Unal, R., and Joyner, C. R., "Application of Taguchi Methods to Dual Mixture Ratio Propulsion System Optimization for SSTO Vehicles," *Journal of Spacecraft and Rockets*, Vol. 29, No. 4, 1992, pp. 453–459.

[26]Cornell, J. A., *How to Apply Response Surface Methodology*, American Society for Quality Control Press, Milwaukee, WI, 1990.

[27]Simberg, R. E., "Space Transportation Comparison Study—NDV Task 11, Phase I, Final Report," Rockwell International, Rockwell Report NA-90-283, Downey, CA, Sept. 1990.

[28]Anon., "Civil Needs Data Base FY90 Version," NASA TM 103321, Aug. 1990.

[29]Kessler, T. L., and Labbee, M. F., "Earth-to-Orbit Delivery Systems; How Future Needs Affect Today's Decisions," AIAA Paper 91-0538, Jan. 1991.

[30]Paster, R. D., and Stohler, S. L., "SSME Evolution for Next-Generation Launch Systems," AIAA Paper 89-2502, July 1989.

[31]Stanley, D. O., and Powell, R. W., "Abort Capabilities of Rocket-Powered Single-Stage Launch Vehicles," *Journal of Spacecraft and Rockets*, Vol. 28, No. 2, 1991, pp. 184–191.

J. A. Martin
Associate Editor